https://doi.org/10.5194/egusphere-2022-1422
Preprint. Discussion started: 12 December 2022

Effects of denitrification on the distributions of trace gas abundances in the polar regions: a model-data comparison

Michael Weimer[1], Douglas E. Kinnison[2], Catherine Wilka[3], and Susan Solomon[1]

[1]Department of Earth, Atmospheric and Planetary Sciences, Massachusetts Institute of Technology, Cambridge, MA, USA
[2]Atmospheric Chemistry Observations & Modeling Laboratory, National Center for Atmospheric Research, Boulder, CO, USA
[3]Department of Earth System Science, Stanford University, Stanford, CA, USA

Correspondence: Michael Weimer (mweimer@mit.edu)

Abstract. Polar stratospheric clouds (PSCs) play a key role in the polar chemistry of the stratosphere. Nitric acid trihydrate (NAT) particles have been shown to lead to denitrification of the lower stratosphere. While the existence of large NAT particles (NAT "rocks") has been verified by many measurements especially in the Northern Hemisphere (NH), most current chemistry-climate models use simplified parametrizations, often based on evaluations in the Southern Hemisphere where the polar vortex is stable enough that accounting for NAT rocks is not as important as in the NH. Here, we evaluate the probability density functions of various gaseous species in the polar vortex using one such model, the Whole Atmosphere Community Climate Model (WACCM), and compare these with measurements by the Michelson Interferometer for Passive Atmospheric Sounding onboard the Environmental Satellite (MIPAS/Envisat) and two ozonesonde stations for a range of years and in both hemispheres. Using the maximum difference between the distributions of MIPAS and WACCM as a measure of coherence, we find better agreement for HNO_3 when reducing the NAT number density from the standard value of 10^{-2} used in this model to $5 \times 10^{-4}\,\mathrm{cm}^{-3}$ for almost all spring seasons during the MIPAS period in both hemispheres. The distributions of $ClONO_2$ and O_3 are not greatly affected by the NAT density. The average difference of WACCM to ozonesondes supports the need to reduce the NAT number density in the model. Therefore, this study suggests to use a NAT number density of $5 \times 10^{-4}\,\mathrm{cm}^{-3}$ for future simulations with WACCM.

1 Introduction

Polar stratospheric clouds (PSCs) have been known for decades to play a key role in explaining the stratospheric ozone hole (Solomon et al., 1986; Solomon, 1999; Tritscher et al., 2021). Reactions on their surfaces lead to activation of chlorine reservoirs, known as chlorine activation. In addition, sedimentation of PSCs result in dehydration and denitrification of the lower stratosphere. Three types of PSCs with different composition and roles have been found to be important: liquid supercooled ternary solution droplets (STS, Carslaw et al., 1994) are major contributors to chlorine activation (e.g., Peter, 1997). Ice PSCs lead to dehydration of the stratosphere (e.g., Kelly et al., 1989). Nitric acid trihydrate particles (NAT) dominate the irreversible removal of nitric acid (HNO_3) from the lower stratosphere via sedimentation, known as denitrification, thus potentially reducing the reformation of chlorine reservoir species which can affect ozone loss (e.g., Waibel et al., 1999).

https://doi.org/10.5194/egusphere-2022-1422
Preprint. Discussion started: 12 December 2022

The existence of NAT particles in the stratosphere has been verified by a variety of airborne measurements (Fahey et al., 1989; Voigt et al., 2000; Fahey, 2001; Molleker et al., 2014; Woiwode et al., 2016). Since the polar vortex in the Southern Hemisphere (SH) generally is more stable than in the Northern Hemisphere (NH) (e.g., Schoeberl et al., 1992), the time period when denitrification can occur is much longer in the SH polar vortex than the NH. On the other hand, denitrification in the NH has been found to occur locally and the role of low-number density large-size NAT particles, so-called NAT rocks, has been discussed and verified by measurements (Fahey, 2001; Fueglistaler et al., 2002; Drdla and Müller, 2012; Adriani et al., 2004; Woiwode et al., 2014, 2016). These large particles can lead to significant sedimentation even on the shorter time scales needed to explain the occurrence of low HNO_3 mixing ratios in the NH spring.

Satellite instruments are able to provide measurements of PSCs and gaseous HNO_3 with daily near-global coverage (Höpfner et al., 2018; Spang et al., 2018; Pitts et al., 2018; Santee et al., 2007; Wespes et al., 2022). Höpfner et al. (2006) found the first evidence of a NAT belt around the Antarctic Continent using the Michelson Interferometer for Passive Atmospheric Sounding (MIPAS) onboard the Environmental Satellite. Therefore, satellite measurements provide a unique opportunity for comparisons of HNO_3 and denitrification with current chemistry-climate models in both hemispheres. They also allow study of the range of the probability distributions in the data for different years and conditions.

Accounting for denitrification is an important process in chemistry-climate models, which is why many parametrizations with different levels of detail have been developed to account for the microphysics and sedimentation of NAT particles in these models (e.g., Wegner et al., 2013; Zhu et al., 2015; Kirner et al., 2011; Weimer et al., 2021). The Whole Atmosphere component of the Community Earth System Model includes a diagnostic parametrization of NAT with a NAT number density set to a global value of $10^{-2}\,\mathrm{cm}^{-3}$ (Wegner et al., 2013). Wilka et al. (2021) found that this value leads to an overestimation of gaseous HNO_3 in the NH for the extraordinarily cold NH winter 2019/2020 in comparison to measurements of the Microwave Limb Sounder. They found a better agreement with the measurements using a NAT number density of $N_{\mathrm{NAT}} = 10^{-5}\,\mathrm{cm}^{-3}$. Here, we investigate this further by applying an adapted version of the method by Zambri et al. (2021) to compare the distributions of various gaseous species within the polar vortex with MIPAS, which provided measurements during 2002 to 2012. MIPAS data is well suited to this task, because it provides high signal to noise local measurements over multiple years in both hemispheres, with good dynamic range; other datasets may also be appropriate but here we use MIPAS for this initial test. Further, using MIPAS and varying the NAT number density of the model, we can also investigate its associated impact on HNO_3, $ClONO_2$ and O_3 for many spring seasons in both hemispheres.

Details about the model and the observation as well as the methods to compare them can be found in Sect. 2. Section 3 shows the comparison between the datasets. Finally, some concluding remarks are given in Sect. 4.

2 Datasets

2.1 WACCM

In this study, we use the Whole Atmosphere component (WACCM6) of the Community Earth System Model (CESM2.1) in Specified Dynamics (SD) mode (Gettelman et al., 2019; Danabasoglu et al., 2020) to compare distributions of the trace gases

https://doi.org/10.5194/egusphere-2022-1422
Preprint. Discussion started: 12 December 2022

Table 1. Simulations in this study. In the "noHetAll" simulation, the heterogeneous reactions are removed apart from the reaction $N_2O_5 + H_2O$.

Simulation	with heterogeneous chemistry?	N_{NAT} (cm^{-3})
HetAll.1e-2	Yes	10^{-2}
noHetAll.5e-4	No	5×10^{-4}
HetAll.5e-4	Yes	5×10^{-4}
HetAll.1e-5	Yes	10^{-5}

with the satellite measurements. The model is relaxed towards the Modern-Era Retrospective Analysis for Research and Applications version 2 (MERRA2, Gelaro et al., 2017). In this study, we use a horizontal resolution of $1.9°\,\mathrm{latitude} \times 2.5°\mathrm{longitude}$ and 88 vertical levels up to about $140\,\mathrm{km}$. In the component set "FWmaSD", a comprehensive chemistry for the middle atmosphere is included, as also used e.g. by Zambri et al. (2021).

Polar stratospheric clouds in WACCM are calculated using a diagnostic parametrization described by Considine et al. (2000), Kinnison et al. (2007) and Wegner et al. (2013). Coexistence of NAT and STS is accounted for by allowing $20\,\%$ of HNO_3 to form NAT whereas the rest is available for STS (Wegner et al., 2013; Solomon et al., 2015). NAT sedimentation, i.e. the vertical redistribution of gaseous HNO_3, is calculated using a simple upwind scheme. The NAT number density is a global parameter in this scheme. Examination of observations of NAT particle number densities (Pitts et al., 2009, 2011) and an emphasis on HNO_3 data for the SH in 2005 led Wegner et al. (2013) to adopt a NAT value of $0.01\,\mathrm{cm}^{-3}$. However, it is important to emphasize that the model's NAT parameterization is subject to multiple simplifications of complex microphysics, so observed NAT particle abundances may therefore not be the best guide for this parameter choice. Here we have had the benefit of the unusual NH year 2020 and have placed more emphasis on both hemispheres to derive a parameterization that better represents the remaining gas phase HNO_3 in the maximum number of years and for both hemispheres.

We performed sensitivity simulations varying the number density of NAT from 10^{-2} to $10^{-5}\,\mathrm{cm}^{-3}$ in the current version 6 of WACCM. We also performed a simulation excluding stratospheric heterogeneous reactions, apart from the reaction $N_2O_5 + H_2O$, to evaluate the impact of heterogeneous processes on the gas-phase species. All simulations are summarized in Table 1. They cover the satellite period starting from 1979 to present.

2.2 MIPAS

The Michelson Interferometer for Passive Atmospheric Sounding (MIPAS) operated in limb geometry on board the Environmental Satellite (Envisat) between July 2002 and April 2012 (Fischer et al., 2008; Chirkov et al., 2016). Envisat was placed in a sun-synchronous polar orbit at an altitude of around $800\,\mathrm{km}$ with more than 14 orbits per day. MIPAS measured a variety of trace gases including HNO_3, $ClONO_2$ and O_3 using a Fourier transform spectrometer in the infrared spectral range between 4.15 and $14.6\,\mu\mathrm{m}$ at tangent altitudes from 7 to $72\,\mathrm{km}$ (Fischer et al., 2008). The spatial resolution was approximately $3\,\mathrm{km}$

https://doi.org/10.5194/egusphere-2022-1422
Preprint. Discussion started: 12 December 2022

in the vertical and 30 km in the horizontal. The spectral resolution was $0.05\,\mathrm{cm}^{-1}$ between 2002 and March 2004. Due to technical issues with the satellite and a corresponding gap of measurements, MIPAS started measuring again in January 2005 with a reduced spectral resolution of $0.12\,\mathrm{cm}^{-1}$.

For this study, we use the V8 level 2 MIPAS retrievals (Kiefer et al., 2021, 2022; Von Clarmann et al., 2009) of HNO_3, $ClONO_2$ and O_3 to compare their distributions with the WACCM simulations. The reported precision in the region between 30 and 150 hPa is $5-15\,\%$ (around 100 pptv) for HNO_3 (Sheese et al., 2016; Castelli et al., 2016; Raspollini et al., 2014; Sheese et al., 2017), $10\,\%$ (around 150 ppbv) for O_3 (Castelli et al., 2016; Sheese et al., 2017; Raspollini et al., 2014) and $7-32\,\%$ ($24-89$ pptv) for $ClONO_2$ (Sheese et al., 2016; Höpfner et al., 2007).

The method used to compare the MIPAS data with WACCM is based on the approach by Zambri et al. (2021). It takes advantage of WACCM's ability to provide output at the locations and times closest to the MIPAS profiles. In combination with interpolation of the MIPAS vertical levels to the WACCM altitudes, this enables a direct comparison of the two datasets. As a result, probability density functions (PDFs) can be evaluated in the spatiotemporal range of interest and compared to the observations.

Since NAT formation and denitrification are strongly temperature-dependent and most efficient at the lowest temperatures, we compute PDFs for profiles inside the polar vortex, determined by MERRA2 using the Nash criterion (Nash et al., 1996). As the sedimentation of the NAT particles takes several weeks (Tabazadeh et al., 2001), the largest effects of denitrification can be expected to be most amplified after the local winter, which is why we restrict our analysis to the early local spring, i.e. 1 February to 15 March in the Northern Hemisphere and 1 September to 15 October in the Southern Hemisphere, and to the pressure range 30 to 150 hPa. Sensitivity studies by changing these two ranges did not affect the main message of the results shown in the next section. In order to make the datasets comparable, we remove the profiles from both WACCM and MIPAS data where negative values occur in the measurements. The number of profiles depends on the area of the polar vortex and differs from year to year. Generally, the number of profiles is larger in the SH due to the larger size of the SH polar vortex compared to the NH.

Zambri et al. (2021) used the Kolomogorov-Smirnov test to evaluate the difference in the PDFs between the model and observations, which uses the number of data points and the maximum difference in the cumulative density functions (CDFs) to check whether the distributions are distinguishable in a statistical sense related to a significance level α. Here, we use the maximum difference in the CDFs "max(d)" of the respective WACCM simulation to MIPAS directly to evaluate the difference in the distributions.

2.3 Ozonesondes

We also compare the WACCM simulations to balloon-borne in-situ measurements of ozonesondes, made available by the World Ozone and Ultraviolet Data Centre. They use an electrochemical concentration cell to measure ozone profiles with a precision of 3 to $5\,\%$ and an uncertainty of about $\pm 10\,\%$ in the pressure range of interest here (Smit et al., 2007). We use ozonesondes of two stations: Eureka in the NH (80.04 °N, 86.18 °W) and Syowa in the SH (69.00 °S, 39.58 °E).

https://doi.org/10.5194/egusphere-2022-1422
Preprint. Discussion started: 12 December 2022

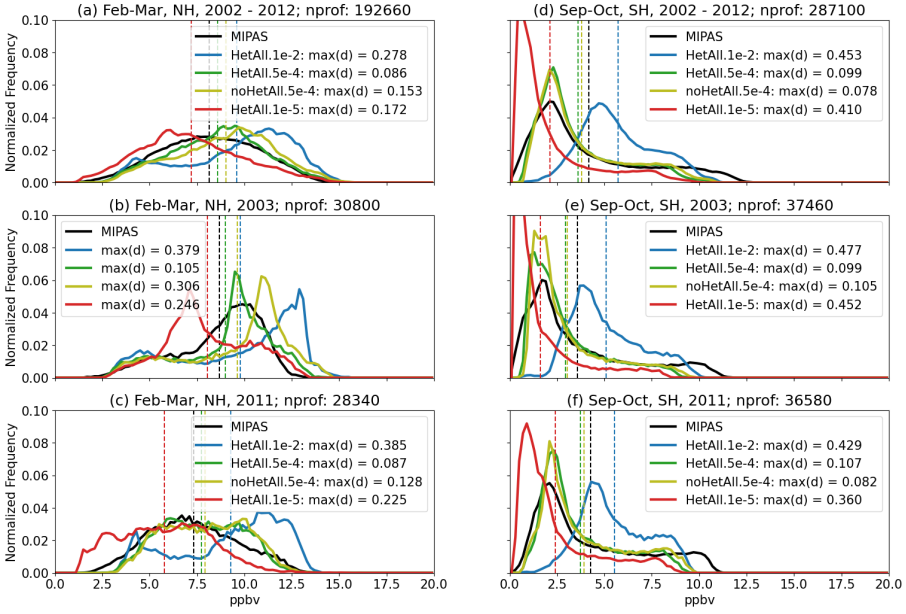

Figure 1. HNO_3 probability density functions within the polar vortex for MIPAS and the sensitivity simulations of WACCM for the NH (left column) and SH (right column) spring months in (a,d) the MIPAS period 2002 to 2012, (b,e) 2003 and (c,f) 2011. Vertical dashed lines show the average volume mixing ratio of the respective simulations. The maximum differences between the CDFs of MIPAS and the respective WACCM simulation are denoted by "max(d)" in the panels.

The method to compare the WACCM simulations with the ozonesonde measurements is similar to Wilka et al. (2021): The data is compared to the daily averaged WACCM ozone concentration at the grid point closest to the respective station. Averages and spread of the differences between WACCM and the observations are evaluated.

3 Impact on the distribution of gas-phase species

Probability density functions of HNO_3 for the whole MIPAS period 2002 to 2012 and for the years 2003 and 2011 are shown in Fig. 1 within the polar vortex in both hemispheres. The blue line corresponds to the simulation with the largest NAT density, the red line shows the simulation with smallest NAT density and the green and yellow lines show the simulations using $N_{\mathrm{NAT}} = 5 \times 10^{-4}\,\mathrm{cm}^{-3}$, with the latter probing turning off all heterogeneous chemistry apart from $N_2O_5 + H_2O$. The black line corresponds to the MIPAS HNO_3 PDF.

Figure 1 demonstrates that the NAT density has a large impact on the PDFs in the model between 30 and 150 hPa. In HetAll.1e-2, larger HNO_3 values are more frequent cpmpared to the other simulations in all the panels. In contrast to this, HetAll.1e-5 underestimates HNO_3 as manifested by a higher frequency at smaller values. The simulation with peak values closest to the MIPAS observations in all panels of Fig. 1 is HetAll.5e-4, indicating that heterogeneous chemistry is relevant and that $N_{\mathrm{NAT}} = 5 \times 10^{-4}\,\mathrm{cm}^{-3}$ leads to PDFs comparable to MIPAS for all years, see also Fig. S1 in the supplement showing

https://doi.org/10.5194/egusphere-2022-1422
Preprint. Discussion started: 12 December 2022

Table 2. Maximum differences of WACCM to MIPAS HNO_3 CDFs ("max(d)" in the figures) for all years, 1 February to 15 March in the NH. Minimum values of each row are highlighted.

Years	HetAll.1e-2	HetAll.5e-4	noHetAll.5e-4	HetAll.1e-5
2002 – 2012	0.278	**0.086**	0.153	0.172
2003	0.379	**0.105**	0.306	0.246
2004	0.187	0.167	0.214	**0.136**
2005	0.283	**0.119**	0.190	0.296
2006	0.155	**0.045**	0.166	0.325
2007	0.297	**0.194**	0.302	0.220
2008	0.443	**0.177**	0.309	0.242
2009	0.148	**0.095**	0.193	0.141
2010	0.319	**0.080**	0.169	0.195
2011	0.385	**0.087**	0.128	0.225
2012	0.226	0.150	0.205	**0.139**

the distributions of all individual years. However, the NAT parametrization in WACCM is not able to capture the minimum and maximum values, especially in the SH where volume mixing ratios as high as $12.5\,\mathrm{ppbv}$ have been measured by MIPAS whereas the largest values in HetAll.5e-4 are around $10\,\mathrm{ppbv}$, e.g. in panel d of Fig. 1.

The overall agreement is also shown by the mean values illustrated by the dashed vertical lines in the figure. The mean HNO_3 value for HetAll.5e-4 is closest to the MIPAS mean value in all the panels, too. In addition, the maximum difference "max(d)" of the 5e-4 simulations is smallest in the shown years compared to the other simulations.

In almost all years, heterogeneous chemistry leads to about $0.5\,\mathrm{ppbv}$ smaller HNO_3 mixing ratios in the NH, see also Fig. S1 in the supplement. In the SH, this effect is not as large as in the NH. Mean and shape of the distributions are similar for noHetAll.5e-4 and HetAll.5e-4.

Since the number of profiles differs from year to year depending on the development of the polar vortex, more weight in the distributions of the whole period 2002 to 2012 (panels a and d in Fig. 1) is given to years with a larger polar vortex. This is why the distributions of all individual years are shown in the supplement (Figs. S1 to S3). As a summary, the max(d) values of the individual years are shown in Tables 2 and 3 for NH and SH, respectively. The simulation with the minimum difference is highlighted for each year. Apart from some exceptions in the NH, the minimum difference occurs for the simulations using $N_{\mathrm{NAT}} = 5 \times 10^{-4}\,\mathrm{cm}^{-3}$. This is another indication that this value improves denitrification and the distribution of HNO_3 in the polar vortex in both hemispheres.

Exceptions are the years 2004 and 2012 in the NH, where the simulation with the smallest NAT density (HetAll.1e-5) shows the minimum differences compared to the MIPAS distribution, see Table 2. In 2004, relatively warm temperatures in the NH stratosphere lead to small denitrification (Manney et al., 2005). As shown in Fig. 2a, this is reflected by the WACCM HNO_3 distributions which do not show large differences when changing the NAT density during that year. There seems to be

https://doi.org/10.5194/egusphere-2022-1422
Preprint. Discussion started: 12 December 2022

Table 3. Same as Table 2, but for the SH spring (1 September to 15 October).

Years	HetAll.1e-2	HetAll.5e-4	noHetAll.5e-4	HetAll.1e-5
2002 – 2012	0.453	0.099	**0.078**	0.410
2002	0.558	0.173	**0.141**	0.642
2003	0.477	**0.099**	0.105	0.452
2005	0.598	**0.095**	0.124	0.559
2006	0.553	**0.141**	0.210	0.366
2007	0.467	0.124	**0.110**	0.404
2008	0.495	0.112	**0.089**	0.432
2009	0.409	0.078	**0.072**	0.290
2010	0.419	0.156	**0.129**	0.425
2011	0.429	0.107	**0.082**	0.360

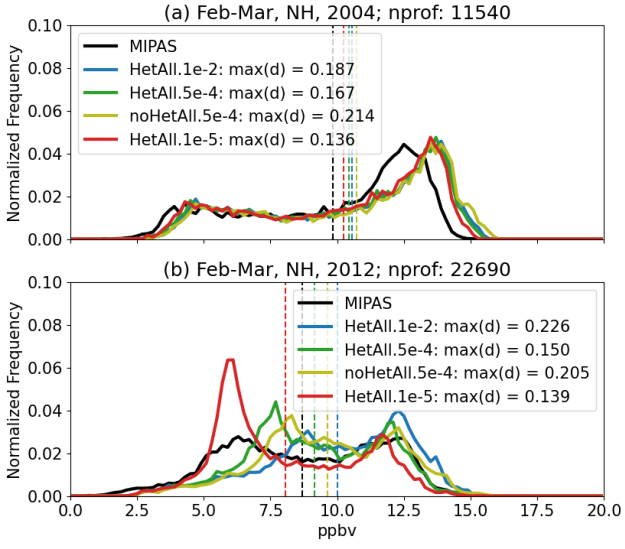

Figure 2. Same as Fig. 1, but for the years (a) 2004 and (b) 2012 in the NH.

a systematic difference between WACCM and MIPAS in this year, though, maybe due to a lower precision of the instrument at that time (Piccolo and Dudhia, 2007). The Arctic winter 2011/2012 was characterized by an early breakdown of the polar vortex at the end of December (Roy and Kuttippurath, 2022), but there is some evidence of large NAT particles during the cold period during December 2011 (Woiwode et al., 2019). This is why the HNO_3 distributions change in WACCM and probably large NAT particles play a larger role in determining the distributions for that year, see Fig. 2b.

Moderate changes due to the different NAT densities can also be found in other species. Figure 3 shows the distributions of chlorine nitrate ($ClONO_2$) for the same years and simulations as in Fig. 1. Both HetAll.1e-2 and HetAll.5e-4 have similar

https://doi.org/10.5194/egusphere-2022-1422
Preprint. Discussion started: 12 December 2022

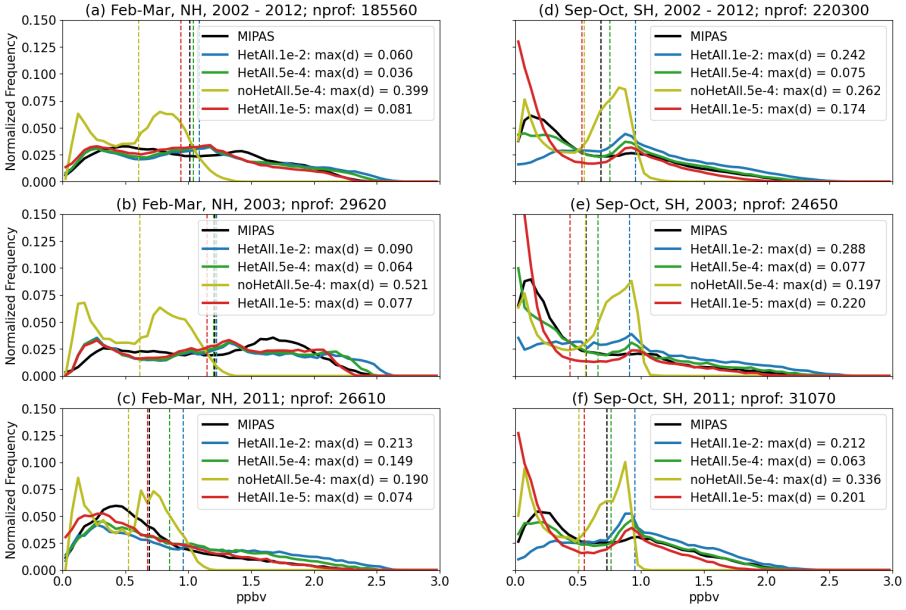

Figure 3. Same as Fig. 1, but for $ClONO_2$.

distributions and max(d) values. Depending on the year, minimum max(d) values occur in both simulations. HetAll.1e-5 seems to slightly underestimate the $ClONO_2$ mixing ratios in both hemispheres, illustrated by higher frequencies of low mixing ratios.

As a result of larger denitrification, impacts on the maximum values in the $ClONO_2$ distributions can be seen in both hemispheres. While the maximum $ClONO_2$ mixing ratios in the NH are closer to the MIPAS distributions using $N_{NAT} = 10^{-5}\,cm^{-3}$, the HetAll.5e-4 simulation captures the maximum values in the SH distributions.

There is also a clear signature of heterogeneous chemistry in the $ClONO_2$ distributions. $ClONO_2$ is formed faster in early spring than HCl (Solomon et al., 2016). Therefore, while the simulation without chemistry noHetAll.5e-4 generally shows $ClONO_2$ volume mixing ratios that are too low compared to MIPAS, it is notable that the maximum values are increased by about 1 ppbv and then are comparable to MIPAS in all simulations with heterogeneous chemistry.

Similar impacts can be seen in the distributions of ozone (O_3), shown in Fig. 4. Ozone volume mixing ratios are about 0.1 ppmv too large in the SH for noHetAll.5e-4 compared to MIPAS. In the NH, the difference is smaller but ozone is still overestimated in the simulation without heterogeneous chemistry.

Wilka et al. (2021) showed that the agreement of WACCM model calculations of Arctic spring ozone losses in 2020 with ozonesonde data was heavily dependent on the denitrification parameterization used in the model, providing an important check. Figure 5 displays comparisons between WACCM and ozonesonde data at Syowa and Eureka for their respective spring seasons for all years between 2002-2012. A figure showing the comparison to Syowa without noHetAll.5e-4 can be found in the supplement (Fig. S4). Similar comparisons are provided for the South Pole in supplemental Fig. S5. Because local

https://doi.org/10.5194/egusphere-2022-1422
Preprint. Discussion started: 12 December 2022

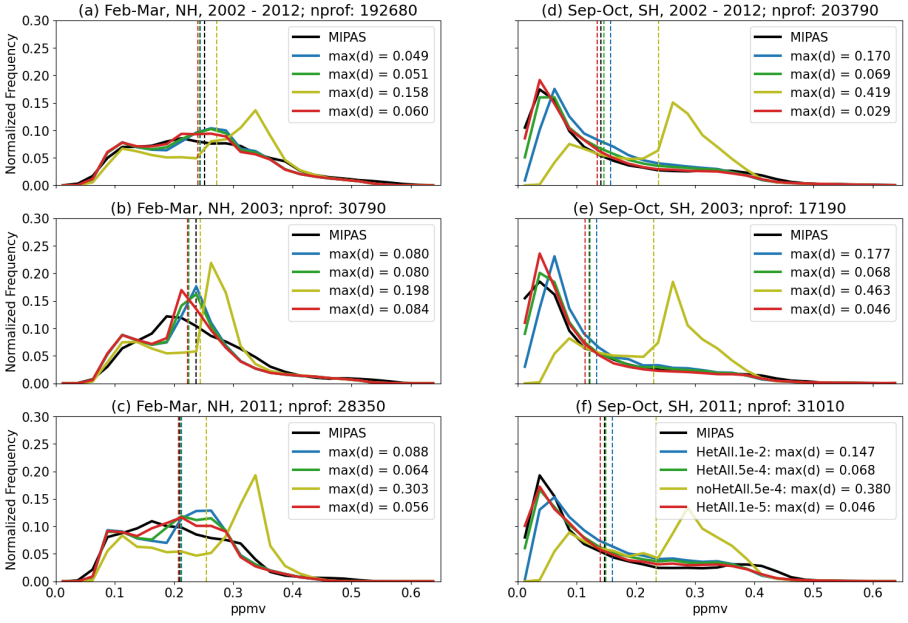

Figure 4. Same as Fig. 1, but for O_3.

Antarctic ozone abundances can drop to values close to zero between about 15-20 km in years with large ozone losses, care must be taken in interpreting percentage differences; we also provide absolute differences for that reason. The Syowa sondes agree considerably better with the model when the NAT number density of $5 \times 10^{-4}\,\mathrm{cm}^{-3}$ or less is used, compared to larger values of this parameter. At Eureka, results are far less sensitive due to smaller ozone losses, except in very cold years (like 2020 shown in Wilka et al., 2021).

In summary, the results in this section showed that the diagnostic parametrization of NAT particles in WACCM is able to reflect the main features in the three key gas-phase species HNO_3, $ClONO_2$ and ozone. When using a reduced NAT particle number density of $N_{\mathrm{NAT}} = 5 \times 10^{-4}\,\mathrm{cm}^{-3}$ compared to the standard WACCM setup, the difference in the cumulative density functions is minimized for almost all spring months of the MIPAS period 2002 to 2012 and the bias between 30 and 150 hPa in comparison to the ozonesondes is reduced. This indicates that $N_{\mathrm{NAT}} = 5 \times 10^{-4}\,\mathrm{cm}^{-3}$ improves the distribution of these species in the polar regions and that it should be used in future WACCM simulations.

4 Discussion and Conclusions

In this study, we investigated the impact of the NAT number density (N_{NAT}) on the distributions of key gaseous species in the WACCM model. We compared probability density functions within the polar vortex with the MIPAS satellite instrument which operated between 2002 and 2012. As a measure of the difference between the distributions of WACCM and MIPAS, we used the maximum difference, max(d), between the cumulative density functions. To identify the impact of NAT on the distributions

https://doi.org/10.5194/egusphere-2022-1422
Preprint. Discussion started: 12 December 2022

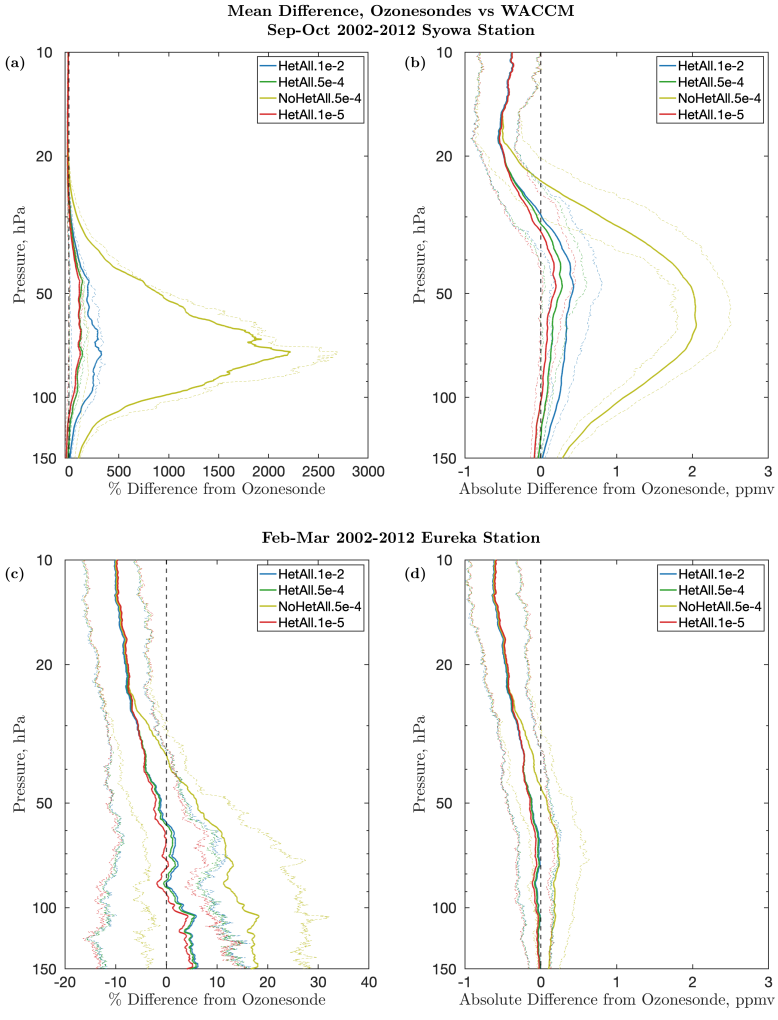

Figure 5. Mean and interquantile (0.25 and 0.75) range of the differences between the respective WACCM simulations and two ozonesonde stations. The first row shows Syowa Station in the Antarctic and the second row shows Eureka Station in the Arctic. For WACCM, the grid point closest to the station is chosen. Average and distributions are taken for all profiles within the MIPAS period and the same months as for the satellite comparison. The left and right columns show the relative and absolute difference to the measurements, respectively.

https://doi.org/10.5194/egusphere-2022-1422
Preprint. Discussion started: 12 December 2022

of the species, we performed sensitivity simulations varying N_{NAT} between 10^{-2} and $10^{-5}\,\mathrm{cm}^{-3}$. In the method applied here to compare the satellite measurements with the model, negative values in the satellite retrievals are cut off, which is why it cannot be used for noisy data (such as N_2O_5 and ClO in MIPAS) and we restricted the analysis to the gaseous species HNO_3, $ClONO_2$ and O_3.

The diagnostic parametrization of NAT in the WACCM model was shown to be able to reproduce the general shape of the MIPAS distributions for almost all years of the MIPAS period in the polar vortices of both hemispheres. There was a general overestimation of gaseous HNO_3, though, when using the standard N_{NAT} of $10^{-2}\,\mathrm{cm}^{-3}$. Reducing this number concentration to $5 \times 10^{-4}\,\mathrm{cm}^{-3}$ was shown to also reduce the differences in the HNO_3 distributions between MIPAS and WACCM for almost all spring seasons in both hemispheres during the MIPAS period. Changes in the distributions of $ClONO_2$ and O_3 due to the new value of N_{NAT} were either negligible or the differences were reduced. Mean differences between ozonesonde profiles and the WACCM simulations at the grid point closest to the sonde stations Syowa and Eureka were also shown to be decreased when reducing N_{NAT}. Therefore, this study suggests the use of $N_{\mathrm{NAT}} = 5 \times 10^{-4}\,\mathrm{cm}^{-3}$ for future simulations.

A simplified parametrization as applied in WACCM cannot capture all features of the distributions of all years. This was demonstrated by the years 2004 and 2012 where differences between the MIPAS and WACCM distributions were increased. Further, there are many uncertainties in the detailed chemistry from one year to another that may also be important for denitrification and ozone loss, including for example volcanic particle inputs, gravity and planetary wave amplitudes, and changes in circulation, to name only a few. It can also be seen that the smallest number density of $10^{-5}\,\mathrm{cm}^{-3}$ is comparable to measurements during the exceptionally cold northern winter 2019/2020 (Wilka et al., 2021). In addition, although overall differences in the PDFs are reduced with $N_{\mathrm{NAT}} = 5 \times 10^{-4}\,\mathrm{cm}^{-3}$, the Kolmogorov-Smirnov test, used e.g. by Zambri et al. (2021), will fail if not using a significance level α that is set to a very small value ($O(10^{-70})$). Therefore, although the differences are decreased, the distributions of MIPAS and WACCM are still different in a statistical sense, probably due to the simplifications in the NAT parametrization of WACCM.

Future studies could apply this methodology to other long-term satellite measurements to evaluate the usage of this new NAT number density for further years. Nevertheless, as a follow-up of the publication by Wilka et al. (2021), we recommend using $N_{\mathrm{NAT}} = 5 \times 10^{-4}\,\mathrm{cm}^{-3}$ for future simulations with WACCM, indicating that NAT rocks play an important role, especially in the NH where we saw the largest impact on changing the NAT number density.

Code and data availability. Instructions for the access to MIPAS data can be found at https://www.imk-asf.kit.edu/english/308.php (last access on 18 November 2022). Instructions how to download CESM version 2 can be found in Danabasoglu et al. (2020). Ozonezonde station data are publicly available through the World Ozone and Ultraviolet Data Center (WOUDC; WMO/GAW Ozone Monitoring Community, 2022). The scripts and data needed to create the figures of this paper can be found at https://g-27eb33.7a577b.6fbd.data.globus.org/ACP_Weimer_2022/ACP_Weimer_2022.tar.gz (last access on 7 December 2022).

https://doi.org/10.5194/egusphere-2022-1422
Preprint. Discussion started: 12 December 2022

Author contributions. MW added the comparison with MIPAS and wrote the first draft of the manuscript. DEK performed the simulations with WACCM used for the comparisons. CW added the comparison to ozonesondes. All authors contributed to prepare the manuscript.

Competing interests. The authors declare that they have no competing interests.

Acknowledgements. Michael Weimer and Douglas E. Kinnison were funded in part by NASA grant 80NSSC19K0952. Susan Solomon was funded in part by grant no. 1906719 of the U.S. National Science Foundation (NSF). We would like to thank Brian Zambri for initiating this work and helping with the comparison to MIPAS. This material is based upon work supported by National Center for Atmospheric Research (NCAR), which is a major facility sponsored by NSF under the Cooperative Agreement 1852977. The CESM project is supported primarily by NSF. We would like to acknowledge support from the Svante cluster at MIT used for the comparison of model and the data, see https://svante.mit.edu/intro.html (last access 18 November 2022) for more information. We would like to acknowledge high-performance computing support from Cheyenne and Casper provided by NCAR's Computational and Information Systems Laboratory (2019), sponsored by NSF.

https://doi.org/10.5194/egusphere-2022-1422
Preprint. Discussion started: 12 December 2022

References

Adriani, A., Massoli, P., Di Donfrancesco, G., Cairo, F., Moriconi, M. L., and Snels, M.: Climatology of polar stratospheric clouds based on lidar observations from 1993 to 2001 over McMurdo Station, Antarctica, J. Geophys. Res.: Atmospheres, 109, 1–17, https://doi.org/10.1029/2004JD004800, 2004.

Carslaw, K. S., Luo, B. P., Clegg, S. L., Peter, T., Brimblecombe, P., and Crutzen, P. J.: Stratospheric aerosol growth and HNO3 gas phase depletion from coupled HNO3 and water uptake by liquid particles, Geophys. Res. Lett., 21, 2479–2482, https://doi.org/10.1029/94GL02799, 1994.

Castelli, E., Ridolfi, M., Carlotti, M., Sinnhuber, B. M., Kirner, O., Kiefer, M., and Dinelli, B. M.: Errors induced by different approximations in handling horizontal atmospheric inhomogeneities in MIPAS/ENVISAT retrievals, Atmos. Meas. Tech., 9, 5499–5508, https://doi.org/10.5194/AMT-9-5499-2016, 2016.

Chirkov, M., Stiller, G. P., Laeng, A., Kellmann, S., Von Clarmann, T., Boone, C. D., Elkins, J. W., Engel, A., Glatthor, N., Grabowski, U., Harth, C. M., Kiefer, M., Kolonjari, F., Krummel, P. B., Linden, A., Lunder, C. R., Miller, B. R., Montzka, S. A., Muhle, J., O'Doherty, S., Orphal, J., Prinn, R. G., Toon, G., Vollmer, M. K., Walker, K. A., Weiss, R. F., Wiegele, A., and Young, D.: Global HCFC-22 measurements with MIPAS: Retrieval, validation, global distribution and its evolution over 2005-2012, Atmos. Chem. Phys., 16, 3345–3368, https://doi.org/10.5194/ACP-16-3345-2016, 2016.

Computational and Information Systems Laboratory: Cheyenne: HPE/SGI ICE XA System (University Community Computing), Tech. rep., National Center for Atmospheric Research, Bolder, CO, https://doi.org/10.5065/D6RX99HX, 2019.

Considine, D. B., Douglass, A. R., Connell, P. S., Kinnison, D. E., and Rotman, D. A.: A polar stratospheric cloud parameterization for the global modeling initiative three-dimensional model and its response to stratospheric aircraft, J. Geophys. Res.: Atmospheres, 105, 3955–3973, https://doi.org/10.1029/1999JD900932, 2000.

Danabasoglu, G., Lamarque, J. F., Bacmeister, J., Bailey, D. A., DuVivier, A. K., Edwards, J., Emmons, L. K., Fasullo, J., Garcia, R., Gettelman, A., Hannay, C., Holland, M. M., Large, W. G., Lauritzen, P. H., Lawrence, D. M., Lenaerts, J. T., Lindsay, K., Lipscomb, W. H., Mills, M. J., Neale, R., Oleson, K. W., Otto-Bliesner, B., Phillips, A. S., Sacks, W., Tilmes, S., van Kampenhout, L., Vertenstein, M., Bertini, A., Dennis, J., Deser, C., Fischer, C., Fox-Kemper, B., Kay, J. E., Kinnison, D., Kushner, P. J., Larson, V. E., Long, M. C., Mickelson, S., Moore, J. K., Nienhouse, E., Polvani, L., Rasch, P. J., and Strand, W. G.: The Community Earth System Model Version 2 (CESM2), J. Adv. Model. Earth Syst., 12, e2019MS001 916, https://doi.org/10.1029/2019MS001916, 2020.

Drdla, K. and Müller, R.: Temperature thresholds for chlorine activation and ozone loss in the polar stratosphere, Ann. Geophys., 30, 1055–1073, https://doi.org/10.5194/ANGEO-30-1055-2012, 2012.

Fahey, D. W.: The Detection of Large HNO3-Containing Particles in the Winter Arctic Stratosphere, Science, 291, 1026–1031, https://doi.org/10.1126/science.1057265, 2001.

Fahey, D. W., Kelly, K. K., Ferry, G. V., Poole, L. R., Wilson, J. C., Murphy, D. M., Loewenstein, M., and Chan, K. R.: In situ measurements of total reactive nitrogen, total water, and aerosol in a polar stratospheric cloud in the Antarctic, J. Geophys. Res., 94, 11 299, https://doi.org/10.1029/JD094iD09p11299, 1989.

Fischer, H., Birk, M., Blom, C., Carli, B., Carlotti, M., von Clarmann, T., Delbouille, L., Dudhia, A., Ehhalt, D., Endemann, M., Flaud, J. M., Gessner, R., Kleinert, A., Koopman, R., Langen, J., López-Puertas, M., Mosner, P., Nett, H., Oelhaf, H., Perron, G., Remedios, J., Ridolfi, M., Stiller, G., and Zander, R.: MIPAS: an instrument for atmospheric and climate research, Atmos. Chem. Phys., 8, 2151–2188, https://doi.org/10.5194/acp-8-2151-2008, 2008.

https://doi.org/10.5194/egusphere-2022-1422
Preprint. Discussion started: 12 December 2022

Fueglistaler, S., Luo, B. P., Voigt, C., Carslaw, K. S., and Peter, T.: NAT-rock formation by mother clouds: A microphysical model study, Atmos. Chem. Phys., 2, 99–101, https://doi.org/10.5194/ACP-2-93-2002, 2002.

Gelaro, R., McCarty, W., Suárez, M. J., Todling, R., Molod, A., Takacs, L., Randles, C. A., Darmenov, A., Bosilovich, M. G., Reichle, R., Wargan, K., Coy, L., Cullather, R., Draper, C., Akella, S., Buchard, V., Conaty, A., da Silva, A. M., Gu, W., Kim, G.-K., Koster, R., Lucchesi, R., Merkova, D., Nielsen, J. E., Partyka, G., Pawson, S., Putman, W., Rienecker, M., Schubert, S. D., Sienkiewicz, M., and Zhao, B.: The Modern-Era Retrospective Analysis for Research and Applications, Version 2 (MERRA-2), J. Clim., 30, 5419–5454, https://doi.org/10.1175/JCLI-D-16-0758.1, 2017.

Gettelman, A., Mills, M. J., Kinnison, D. E., Garcia, R. R., Smith, A. K., Marsh, D. R., Tilmes, S., Vitt, F., Bardeen, C. G., McInerny, J., Liu, H. L., Solomon, S. C., Polvani, L. M., Emmons, L. K., Lamarque, J. F., Richter, J. H., Glanville, A. S., Bacmeister, J. T., Phillips, A. S., Neale, R. B., Simpson, I. R., DuVivier, A. K., Hodzic, A., and Randel, W. J.: The Whole Atmosphere Community Climate Model Version 6 (WACCM6), J. Geophys. Res.: Atmospheres, 124, 12 380–12 403, https://doi.org/10.1029/2019JD030943, 2019.

Höpfner, M., Larsen, N., Spang, R., Luo, B. P., Ma, J., Svendsen, S. H., Eckermann, S. D., Knudsen, B., Massoli, P., Cairo, F., Stiller, G., v. Clarmann, T., and Fischer, H.: MIPAS detects Antarctic stratospheric belt of NAT PSCs caused by mountain waves, Atmos. Chem. Phys., 6, 1221–1230, https://doi.org/10.5194/acp-6-1221-2006, 2006.

Höpfner, M., Von Clarmann, T., Fischer, H., Funke, B., Glatthor, N., Grabowski, U., Kellmann, S., Kiefer, M., Linden, A., Milz, M., Steck, T., Stiller, G. P., Bernath, P., Blom, C. E., Blumenstock, T., Boone, C., Chance, K., Coffey, M. T., Friedl-Vallon, F., Griffith, D., Hannigan, J. W., Hase, F., Jones, N., Jucks, K. W., Keim, C., Kleinert, A., Kouker, W., Liu, G. Y., Mahieu, E., Mellqvist, J., Mikuteit, S., Notholt, J., Oelhaf, H., Piesch, C., Reddmann, T., Ruhnke, R., Schneider, M., Strandberg, A., Toon, G., Walker, K. A., Warneke, T., Wetzel, G., Wood, S., and Zander, R.: Validation of MIPAS ClONO2 measurements, Atmos. Chem. Phys., 7, 257–281, https://doi.org/10.5194/ACP-7-257-2007, 2007.

Höpfner, M., Deshler, T., Pitts, M., Poole, L., Spang, R., Stiller, G., and von Clarmann, T.: The MIPAS/Envisat climatology (2002–2012) of polar stratospheric cloud volume density profiles, Atmos. Meas. Tech., 11, 5901–5923, https://doi.org/10.5194/amt-11-5901-2018, 2018.

Kelly, K. K., Tuck, A. F., Murphy, D. M., Proffitt, M. H., Fahey, D. W., Jones, R. L., McKenna, D. S., Loewenstein, M., Podolske, J. R., Strahan, S. E., Ferry, G. V., Chan, K. R., Vedder, J. F., Gregory, G. L., Hypes, W. D., McCormick, M. P., Browell, E. V., and Heidt, L. E.: Dehydration in the lower Antarctic stratosphere during late winter and early spring, 1987, J. Geophys. Res., 94, 11 317, https://doi.org/10.1029/JD094iD09p11317, 1989.

Kiefer, M., von Clarmann, T., Funke, B., García-Comas, M., Glatthor, N., Grabowski, U., Kellmann, S., Kleinert, A., Laeng, A., Linden, A., López-Puertas, M., Marsh, D. R., and Stiller, G. P.: IMK/IAA MIPAS temperature retrieval version 8: nominal measurements, Atmos. Meas. Tech., 14, 4111–4138, https://doi.org/10.5194/amt-14-4111-2021, 2021.

Kiefer, M., von Clarmann, T., Funke, B., Garcia-Comas, M., Glatthor, N., Grabowski, U., Höpfner, M., Kellmann, S., Laeng, A., Linden, A., Lopez-Puertas, M., and Stiller, G.: Version 8 IMK/IAA MIPAS ozone profiles: nominal observation mode, Atmos. Meas. Tech. Discuss., 2022, 1–30, https://doi.org/10.5194/amt-2022-257, under review, 2022.

Kinnison, D. E., Brasseur, G. P., Walters, S., Garcia, R. R., Marsh, D. R., Sassi, F., Harvey, V. L., Randall, C. E., Emmons, L., Lamarque, J. F., Hess, P., Orlando, J. J., Tie, X. X., Randel, W., Pan, L. L., Gettelman, A., Granier, C., Diehl, T., Niemeier, U., and Simmons, A. J.: Sensitivity of chemical tracers to meteorological parameters in the MOZART-3 chemical transport model, J. Geophys. Res.: Atmospheres, 112, 20 302, https://doi.org/10.1029/2006JD007879, 2007.

Kirner, O., Ruhnke, R., Buchholz-Dietsch, J., Jöckel, P., Brühl, C., and Steil, B.: Simulation of polar stratospheric clouds in the chemistry-climate-model EMAC via the submodel PSC, Geosci. Model Dev., 4, 169–182, https://doi.org/10.5194/gmd-4-169-2011, 2011.

https://doi.org/10.5194/egusphere-2022-1422
Preprint. Discussion started: 12 December 2022

Manney, G. L., Krüger, K., Sabutis, J. L., Sena, S. A., and Pawson, S.: The remarkable 2003–2004 winter and other recent warm winters in the Arctic stratosphere since the late 1990s, J. Geophys. Res.: Atmospheres, 110, 1–14, https://doi.org/10.1029/2004JD005367, 2005.

Molleker, S., Borrmann, S., Schlager, H., Luo, B., Frey, W., Klingebiel, M., Weigel, R., Ebert, M., Mitev, V., Matthey, R., Woiwode, W., Oelhaf, H., Dörnbrack, A., Stratmann, G., Grooß, J.-U., Günther, G., Vogel, B., Müller, R., Krämer, M., Meyer, J., and Cairo, F.: Microphysical properties of synoptic-scale polar stratospheric clouds: in situ measurements of unexpectedly large HNO3-containing particles in the Arctic vortex, Atmos. Chem. Phys., 14, 10 785–10 801, https://doi.org/10.5194/acp-14-10785-2014, 2014.

Nash, E. R., Newman, P. A., Rosenfield, J. E., and Schoeberl, M. R.: An objective determination of the polar vortex using Ertel's potential vorticity, J. Geophys. Res.: Atmospheres, 101, 9471–9478, https://doi.org/10.1029/96JD00066, 1996.

Peter, T.: Microphysics and heterogeneous chemistry of polar stratospheric clouds, Annu. Rev. Phys. Chem., 48, 785–822, https://doi.org/10.1146/annurev.physchem.48.1.785, 1997.

Piccolo, C. and Dudhia, A.: Precision validation of MIPAS-Envisat products, Atmos. Chem. Phys., 7, 1915–1923, https://doi.org/10.5194/ACP-7-1915-2007, 2007.

Pitts, M. C., Poole, L. R., and Thomason, L. W.: CALIPSO polar stratospheric cloud observations: second-generation detection algorithm and composition discrimination, Atmos. Chem. Phys., 9, 7577–7589, https://doi.org/10.5194/acp-9-7577-2009, 2009.

Pitts, M. C., Poole, L. R., Dörnbrack, A., and Thomason, L. W.: The 2009–2010 Arctic polar stratospheric cloud season: a CALIPSO perspective, Atmos. Chem. Phys., 11, 2161–2177, https://doi.org/10.5194/acp-11-2161-2011, 2011.

Pitts, M. C., Poole, L. R., and Gonzalez, R.: Polar stratospheric cloud climatology based on CALIPSO spaceborne lidar measurements from 2006 to 2017, Atmos. Chem. Phys., 18, 10 881–10 913, https://doi.org/10.5194/acp-18-10881-2018, 2018.

Raspollini, P., Arnone, E., Barbara, F., Carli, B., Castelli, E., Ceccherini, S., Dinelli, B. M., Dudhia, A., Kiefer, M., Papandrea, E., and Ridolfi, M.: Comparison of the MIPAS products obtained by four different level 2 processors, Ann. Geophys., 56, https://doi.org/10.4401/ag-6338, 2014.

Roy, R. and Kuttippurath, J.: The dynamical evolution of Sudden Stratospheric Warmings of the Arctic winters in the past decade 2011–2021, SN Applied Sciences, 4, 1–12, https://doi.org/10.1007/S42452-022-04983-4/TABLES/1, 2022.

Santee, M. L., Lambert, A., Read, W. G., Livesey, N. J., Cofield, R. E., Cuddy, D. T., Daffer, W. H., Drouin, B. J., Froidevaux, L., Fuller, R. A., Jarnot, R. F., Knosp, B. W., Manney, G. L., Perun, V. S., Snyder, W. V., Stek, P. C., Thurstans, R. P., Wagner, P. A., Waters, J. W., Muscari, G., de Zafra, R. L., Dibb, J. E., Fahey, D. W., Popp, P. J., Marcy, T. P., Jucks, K. W., Toon, G. C., Stachnik, R. A., Bernath, P. F., Boone, C. D., Walker, K. A., Urban, J., and Murtagh, D.: Validation of the Aura Microwave Limb Sounder HNO3 measurements, J. Geophys. Res.: Atmospheres, 112, 24–40, https://doi.org/10.1029/2007JD008721, 2007.

Schoeberl, M. R., Lait, L. R., Newman, P. A., and Rosenfield, J. E.: The structure of the polar vortex, J. Geophys. Res.: Atmospheres, 97, 7859–7882, https://doi.org/10.1029/91JD02168, 1992.

Sheese, P. E., Walker, K. A., Boone, C. D., McLinden, C. A., Bernath, P. F., Bourassa, A. E., Burrows, J. P., Degenstein, D. A., Funke, B., Fussen, D., Manney, G. L., Thomas McElroy, C., Murtagh, D., Randall, C. E., Raspollini, P., Rozanov, A., Russell, J. M., Suzuki, M., Shiotani, M., Urban, J., Von Clarmann, T., and Zawodny, J. M.: Validation of ACE-FTS version 3.5 NOy species profiles using correlative satellite measurements, Atmos. Meas. Tech., 9, 5781–5810, https://doi.org/10.5194/AMT-9-5781-2016, 2016.

Sheese, P. E., Walker, K. A., Boone, C. D., Bernath, P. F., Froidevaux, L., Funke, B., Raspollini, P., and von Clarmann, T.: ACE-FTS ozone, water vapour, nitrous oxide, nitric acid, and carbon monoxide profile comparisons with MIPAS and MLS, J. Quant. Spectrosc. Radiat. Transf., 186, 63–80, https://doi.org/10.1016/J.JQSRT.2016.06.026, 2017.

https://doi.org/10.5194/egusphere-2022-1422
Preprint. Discussion started: 12 December 2022

Smit, H. G. J., Straeter, W., Johnson, B. J., Oltmans, S. J., Davies, J., Tarasick, D. W., Hoegger, B., Stubi, R., Schmidlin, F. J., Northam, T., Thompson, A. M., Witte, J. C., Boyd, I., and Posny, F.: Assessment of the performance of ECC-ozonesondes under quasi-flight conditions in the environmental simulation chamber: Insights from the Juelich Ozone Sonde Intercomparison Experiment (JOSIE), J. Geophys. Res.: Atmospheres, 112, https://doi.org/https://doi.org/10.1029/2006JD007308, 2007.

Solomon, S.: Stratospheric ozone depletion: A review of concepts and history, Rev. Geophys., 37, 275–316, https://doi.org/10.1029/1999RG900008, 1999.

Solomon, S., Garcia, R. R., Rowland, F. S., and Wuebbles, D. J.: On the depletion of Antarctic ozone, Nature, 321, 755–758, https://doi.org/10.1038/321755a0, 1986.

Solomon, S., Kinnison, D., Bandoro, J., and Garcia, R.: Simulation of polar ozone depletion: An update, J. Geophys. Res.: Atmospheres, 120, 7958–7974, https://doi.org/10.1002/2015JD023365, 2015.

Solomon, S., Kinnison, D., Garcia, R. R., Bandoro, J., Mills, M., Wilka, C., Neely, R. R., Schmidt, A., Barnes, J. E., Vernier, J. P., and Höpfner, M.: Monsoon circulations and tropical heterogeneous chlorine chemistry in the stratosphere, Geophys. Res. Lett., 43, 624–12, https://doi.org/10.1002/2016GL071778, 2016.

Spang, R., Hoffmann, L., Müller, R., Grooß, J.-U., Tritscher, I., Höpfner, M., Pitts, M., Orr, A., and Riese, M.: A climatology of polar stratospheric cloud composition between 2002 and 2012 based on MIPAS/Envisat observations, Atmos. Chem. Phys., 18, 5089–5113, https://doi.org/10.5194/acp-18-5089-2018, 2018.

Tabazadeh, A., Jensen, E. J., Toon, O. B., Drdla, K., and Schoeberl, M. R.: Role of the Stratospheric Polar Freezing Belt in Denitrification, Science, 291, 2591–2594, https://doi.org/10.1126/science.1057228, 2001.

Tritscher, I., Pitts, M. C., Poole, L. R., Alexander, S. P., Cairo, F., Chipperfield, M. P., Grooß, J., Höpfner, M., Lambert, A., Luo, B., Molleker, S., Orr, A., Salawitch, R., Snels, M., Spang, R., Woiwode, W., and Peter, T.: Polar Stratospheric Clouds: Satellite Observations, Processes, and Role in Ozone Depletion, Rev. Geophys., 59, e2020RG000 702, https://doi.org/10.1029/2020RG000702, 2021.

Voigt, C., Schreiner, J., Kohlmann, A., Zink, P., Mauersberger, K., Larsen, N., Deshler, T., Kroger, C., Rosen, J., Adriani, A., Cairo, F., Di Donfrancesco, G., Viterbin, M., Ovarlez, J., Ovarlez, H., David, C., and Dornbrack, A.: Nitric Acid Trihydrate (NAT) in Polar Stratospheric Clouds, Science, 290, 1756–1758, https://doi.org/10.1126/SCIENCE.290.5497.1756, 2000.

Von Clarmann, T., Höpfner, M., Kellmann, S., Linden, A., Chauhan, S., Funke, B., Grabowski, U., Glatthor, N., Kiefer, M., Schieferdecker, T., Stiller, G. P., and Versick, S.: Retrieval of temperature, H2O, O3, HNO3, CH4, N2O, ClONO2 and ClO from MIPAS reduced resolution nominal mode limb emission measurements, Atmos. Meas. Tech., 2, 159–175, https://doi.org/10.5194/AMT-2-159-2009, 2009.

Waibel, A. E., Peter, T., Carslaw, K. S., Oelhaf, H., Wetzel, G., Crutzen, P. J., Pöschl, U., Tsias, A., Reimer, E., and Fischer, H.: Arctic Ozone Loss Due to Denitrification, Science, 283, 2064–2069, https://doi.org/10.1126/science.283.5410.2064, 1999.

Wegner, T., Kinnison, D. E., Garcia, R. R., and Solomon, S.: Simulation of polar stratospheric clouds in the specified dynamics version of the whole atmosphere community climate model, J. Geophys. Res.: Atmospheres, 118, 4991–5002, https://doi.org/10.1002/jgrd.50415, 2013.

Weimer, M., Buchmüller, J., Hoffmann, L., Kirner, O., Luo, B., Ruhnke, R., Steiner, M., Tritscher, I., and Braesicke, P.: Mountain-wave-induced polar stratospheric clouds and their representation in the global chemistry model ICON-ART, Atmos. Chem. Phys., 21, 9515–9543, https://doi.org/10.5194/acp-21-9515-2021, 2021.

Wespes, C., Ronsmans, G., Clarisse, L., Solomon, S., Hurtmans, D., Clerbaux, C., and Coheur, P.-F.: Polar stratospheric nitric acid depletion surveyed from a decadal dataset of IASI total columns, Atmos. Chem. Phys., 22, 10 993–11 007, https://doi.org/10.5194/ACP-22-10993-2022, 2022.

https://doi.org/10.5194/egusphere-2022-1422
Preprint. Discussion started: 12 December 2022

Wilka, C., Solomon, S., Kinnison, D., and Tarasick, D.: An Arctic ozone hole in 2020 if not for the Montreal Protocol, Atmos. Chem. Phys., 21, 15 771–15 781, https://doi.org/10.5194/ACP-21-15771-2021, 2021.

WMO/GAW Ozone Monitoring Community: World Meteorological Organization-Global Atmosphere Watch Program (WMO-GAW): Ozone, World Ozone and Ultraviolet Radiation Data Centre (WOUDC) [data set], https://doi.org/10.14287/10000001, 2022.

Woiwode, W., Grooß, J.-U., Oelhaf, H., Molleker, S., Borrmann, S., Ebersoldt, A., Frey, W., Gulde, T., Khaykin, S., Maucher, G., Piesch, C., and Orphal, J.: Denitrification by large NAT particles: the impact of reduced settling velocities and hints on particle characteristics, Atmos. Chem. Phys., 14, 11 525–11 544, https://doi.org/10.5194/acp-14-11525-2014, 2014.

Woiwode, W., Höpfner, M., Bi, L., Pitts, M. C., Poole, L. R., Oelhaf, H., Molleker, S., Borrmann, S., Klingebiel, M., Belyaev, G., Ebersoldt, A., Griessbach, S., Grooß, J.-U., Gulde, T., Krämer, M., Maucher, G., Piesch, C., Rolf, C., Sartorius, C., Spang, R., and Orphal, J.: Spectroscopic evidence of large aspherical β-NAT particles involved in denitrification in the December 2011 Arctic stratosphere, Atmos. Chem. Phys., 16, 9505–9532, https://doi.org/10.5194/acp-16-9505-2016, 2016.

Woiwode, W., Höpfner, M., Bi, L., Khosrawi, F., and Santee, M. L.: Vortex-Wide Detection of Large Aspherical NAT Particles in the Arctic Winter 2011/12 Stratosphere, Geophys. Res. Lett., 46, 13 420–13 429, https://doi.org/10.1029/2019GL084145, 2019.

Zambri, B., Kinnison, D. E., and Solomon, S.: Subpolar Activation of Halogen Heterogeneous Chemistry in Austral Spring, Geophys. Res. Lett., 48, e2020GL090 036, https://doi.org/10.1029/2020GL090036, 2021.

Zhu, Y., Toon, O. B., Lambert, A., Kinnison, D. E., Brakebusch, M., Bardeen, C. G., Mills, M. J., and English, J. M.: Development of a Polar Stratospheric Cloud Model within the Community Earth System Model using constraints on Type I PSCs from the 2010-2011 Arctic winter, J. Adv. Model. Earth Syst., 7, 551–585, https://doi.org/10.1002/2015MS000427, 2015.